Proceedings of the ASME XXXX International Design Engineering Technical Conferences & Computers and Information in Engineering Conference
IDETC/CIE XXXX
August XX-September XX, XXXX, San Diego, USA

DETCXXXX/MESA-XXXXX

MODELLING THE AXIS DRIFT OF SHORT WIRE FLEXURES AND INCREASING THEIR SUPPORT STIFFNESS USING POLYMERS

B. Daan
Dept. of Precision and Microsystems Engineering
Delft University of Technology
Delft, 2628 CD, The Netherlands
B.Daan@student.tudelft.nl

J. Rommers
J.L. Herder
Dept. of Precision and Microsystems Engineering
Delft University of Technology
Delft, 2628 CD, The Netherlands
J.Rommers@tudelft.nl - J.L.Herder@tudelft.nl

ABSTRACT

For steel flexures, complex geometries are required to reach high support stiffness and limit axis drift over large ranges of motion. These complex flexures are expensive and difficult to manufacture. This paper presents a method of designing short, polymer wire flexures with high support stiffness and modelling their axis drift using a novel method, the arc method. The arc method is validated against finite element methods (FEM) and physical tests, showing at least a factor 10 lower error than existing pseudo-rigid-body models (PRBM) at 70° *deflection, while maintaining a simple modelling approach. The use of polymers increases support stiffness of wire flexures by a factor 7800 with respect steel at* 70° *deflection, even though the material stiffness is substantially lower. This is due to the large allowed strain of polymers increasing the possible diameter by a factor 110.*

1 INTRODUCTION

The applications for compliant mechanisms range from the hinge of a shampoo bottle to the highest precision mechanisms. Flexures for precision applications are normally made from steel or other metals because of their predictability [1]. Flexures for consumer products are mostly made of polymer flexures, due to their ease of manufacturing. The use of polymer flexures in precision applications is still a mostly unresearched field, as polymers suffer from low repeatability and high creep. However, they allow for very large strain compared to steel.

With steel flexures, because of their low allowed strain, complex geometries are required to create high support stiffness over large ranges of motion [2]. But these complex flexures are expensive to manufacture and difficult to clean. Contrarily, as polymers allow for larger strain, using them for compliant joints allow thicker flexures for the same range of motion. This could result in high support stiffness over a large range of motion with simple geometries, such as the short wire flexure used as a two degree of freedom (2DOF) small-length flexural pivot.

A problem with simple flexures such as the short wire is that they exhibit axis drift when bending [3]. For rigid body joints, the rotation point or axis is defined by the shape of the joint and does not move when rotating. In more complex flexure designs, axis drift can be mitigated to some extent [4]. However, axis drift of a flexure has no influence on the repeatability of the flexure, but can have an effect on the accuracy of the system if the amount of axis drift is not known. The use of a feedback loop in the control system can correct for low accuracy to some extent, but a higher accuracy can then still decrease overshoot or settling time of the system [5]. To mitigate the accuracy loss due to axis drift, the feed-forward model of the system has to include this axis drift of the flexure when calculating the outputs of the system.

To model the axis drift of a compliant joint Pseudo Rigid Body Modelling (PRBM) or the Finite Element Method (FEM) is commonly used. In PRBM, flexure joints are replaced by revolute joints coupled with a torsional spring. PRBM does not model any axis drift and thus introduces an error [6]. As steel

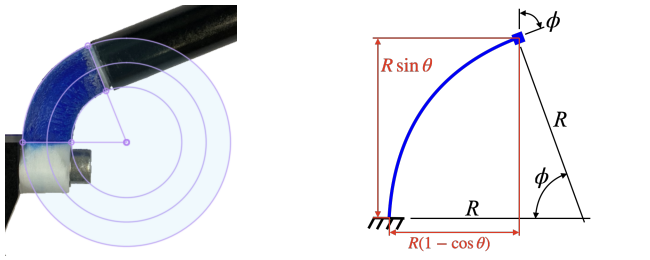

(a) A TPU Flexure bent to 70° showing circular deformation

(b) A schematic drawing of arc method with the calculated endpoint positions

FIGURE 1: A TPU flexure and its arc method equivalent

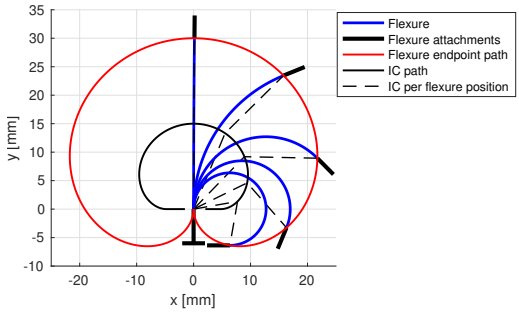

FIGURE 2: The endpoint path (red) of a flexure with a fixed arc length bending to $\pm 360°$, with some flexure positions drawn in blue. The IC path drawn in black, with dotted lines showing IC the position per flexure position.

wire flexures are mostly implemented for small deflection angles, where the effect of axis drift is small, PRBM could still offer high enough accuracy. However, if polymer flexures such as researched in this paper allow for a large range of motion, the error of PRBM increases. Multiple revolute joints per flexure instead of one reduces the error but increases complexity. Howell proposes a solution for this, an optimised single revolute joint position per loading condition, called the characteristic pivot [1]. For this method, however, the loading condition needs to be known, and an angle error is introduced at the endpoint of the flexure. FEM simulates the deflection of a flexure accurately, but a separate simulation for each flexure and bend angle would be required, resulting in large lookup tables, quickly increasing complexity. A simple analytic model for wire flexures for a large range of motion is not yet available.

This paper aims to develop a simple analytic model to accurately model the axis drift of wire flexures used as 2DOF small-length flexural pivots for a large range of motion. To increase robustness and precision of the flexure, the use of polymers for the design of wire flexures with high support stiffness for this large range of motion is investigated.

The structure of this paper is as follows. In section 2, an analytic model named arc method is developed for the axis drift of wire flexures. In section 3, the support stiffness and differences between a steel and polymer wire flexure are investigated. In section 4, the results for both of these methods are presented, after which they are discussed in section 5. Finally, conclusions are presented in section 6.

2 THE ARC METHOD

In section 2.1 a new simple way of modelling wire flexures is proposed, the arc method, after which a technique for implementing this method into kinematic models is given in section 2.2. Finally, it is compared to existing PRBM in section 2.3.

2.1 Modelling Axis Drift With The Arc Method

The arc method uses three theories for cantilever beams to model wire flexures. First, if a cantilever beam is bent by a moment on its free endpoint, the shape of the flexure follows a circular arc, as both the moment and area moment of inertia is constant over the length of the flexure. Second, the neutral axis, which is the axis that does not see any strain or longitudinal forces during bending, does not change length. Third, as the cross-section of a wire flexure is symmetric, the neutral axis lies in the centre of the flexure. Thus, a wire flexure of length L bent by a moment to an angle ϕ can be modelled by a circular arc at its centre line with a constant length L and an angle ϕ. This modelling approach we call the arc method. Figure 1a shows a bent wire flexure made from thermoplastic polyurethane (TPU), and its arc method equivalent in figure 1b. Based on the radius of curvature, which for an arc of known length is specified by $R = \frac{L}{\phi}$, the positions of the endpoint of an arc can easily be found, as also shown in figure 1b.

Any external force deviates the flexure from this arc, as this introduces compression, shear, and an unequal bending moment over the length of the flexure. A high support stiffness can decrease this effect, as will be investigated in section 3. External forces will not be taken into account in this section.

Figure 2 shows the path of the endpoint of the flexure for different deformation angles calculated with the arc method. Also drawn in this figure is the centrode, or path of the instant centre of rotation (IC) of this flexure. The IC is the point around which the rigid body connected to the flexure pivots at each instant. The IC must lie on the line perpendicular to the midpoint of the flexure, as the flexure is symmetrical around this line. The IC can then be determined by intersecting a line perpendicular to the velocity vector of the endpoint with this middle line. The path of the endpoint is known, and the velocity vector must always lie tangent to the path. The migrating IC shows the axis drift of the flexure.

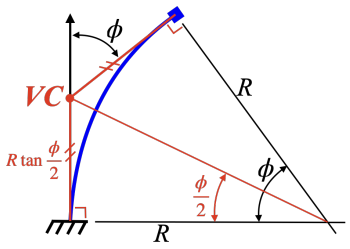

FIGURE 3: The definition of the virtual centre (VC) for a bent flexure. This definition works both in 2D, as depicted here, and in 3D. The VC always lies along the vector tangent to the base of the flexure, depicted in this figure by the black arrow pointed upwards.

2.2 Using The Arc Method For Kinematic Models

With an arc of known length in between each of the rigid bodies, the kinematic model is fully defined and can thus be solved. This means the kinematics of a complex, multi-flexure system can be accurately modelled. To make this method easier to implement, a virtual centre (VC) can be added to the system. This centre is an intersection of the two tangent lines to each of endpoints of the flexures, as can be seen in figure 3. It is important to note that this is not the same as the IC of the flexure, which can be seen in figure 2. Using this VC to solve the system changes the multi flexure model back into a more PRBM like system, but implementing shifting rotation pivots. Two things make this VC well suited for solving the system in comparison to working with the arc method directly or using the IC. First, the VC shifts along a single vector for every deflection angle, as it always lies on the tangent at the base of the flexure. Second, the point is easily calculated based on the deflection angle ϕ of the flexure. Looking again at figure 3, the distance between the base of the flexure and the VC is defined as $R \cdot \tan \frac{\phi}{2}$.

A drawback of using the arc method and VC however, is that due to the shifting rotation pivots the distance between the pivots is dependent on the deflection angle. This increased complexity can result in a necessity for an iterative solver in some systems.

2.3 Comparing The Arc Method To PRBM

For PRBM methods with a single rotation pivot, three methods are found in literature. One has the pivot at the base of the flexure, one centred on the flexure, one at a characteristic pivot location based on the loading condition. Each draws a different circle for the endpoint of the flexure, which are all depicted in figure 4. To find the characteristic pivot, Howell matches the path of the endpoint per loading condition to a circle to minimise the error [1]. For a flexure with an applied moment, a circle with a radius of 0.7346 matches the path best. To then match the deflection rate, an angle coefficient is used, in this case 1.5164. This means that for a flexure angle of 1.5164° degrees,

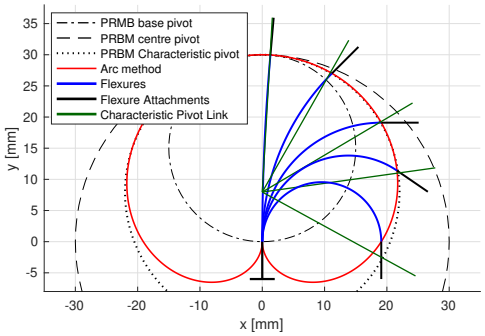

FIGURE 4: The comparison between the arc method and three PRBM approximations. One with the pivot at the base of the flexure, one at the centre of the flexure and one at the characteristic pivot. Flexure shapes for different deflection angles are also shown in blue, as well as the characteristic pivot with angle coefficient in green. The angles for these are: 5°, 45°, 90°, 124.4°, and 180°. 124.4° is the maximum angle for which Howell specifies a position error of less then 0.5% of the tip deflection.

the PRBM linkage has an angle of 1°. Figure 4 shows the green lines modelled by the characteristic pivot with angle coefficient almost intersecting the endpoints of the flexure modelled by the arc method. However, the approximations necessary for the characteristic pivot add complexity compared to the arc method. Next to this, as the arc method describes the exact way a wire flexure deforms due to a moment, the characteristic pivot is also less accurate. The drawbacks of the characteristic pivot only increase when the body connected to the flexure has to be modelled, as the angle coefficient creates an angle error at the endpoint of the flexure. This error can also be seen in figure 4, where the actual flexure attachment in black has a different angle than the characteristic pivot link in green.

3 SUPPORT STIFFNESS

Deflections caused by external forces can cause an error in the prediction of the arc method. A high support stiffness decreases this error, increasing the robustness of the model. In section 3.1, the support stiffness for a short wire flexure is defined, after which the effect of material strain is investigated in section 3.2. The support stiffness is then modelled in section 3.3.

3.1 Defining Support Stiffness For A Wire Flexure

For a short wire flexure used as a 2DOF small-length flexural pivot, we define the support stiffness to be the following: The stiffness against loading at the endpoint tangent to the flexure while constraining its rotation, as is illustrated in figure 5. This is based on the loading of a ball joint in its most common use, a truss-like setup where a rod has a ball joint at either end, resulting

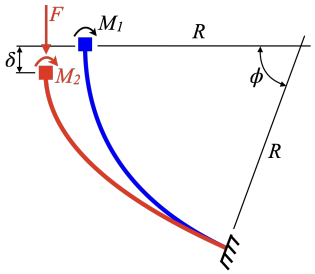

FIGURE 5: Support stiffness F/δ of a bend short wire flexure, where ϕ is the deflection angle of the flexure. Moment M_1 is the bending moment necessary for this deflection angle. Moment M_2 consists of the initial bending moment plus the constraining moment to keep the angle ϕ when loading.

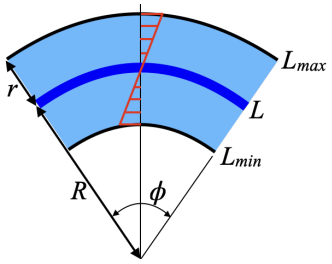

FIGURE 6: A bend wire flexure to angle ϕ. The undeformed length of the flexure is L, which is still the case at the centre-line. The elongated outside of the flexure has an length of L_{max}, while the compressed inside has a length of L_{min}. The radius of curvature is R, and the radius of the flexure itself is r.

in a two force member. The rod can only be in pure compression or tension, but the mechanism does input a certain deflection angle on the ball joints. In such a system, the distance between the two joints constrains the mechanism, so the deflection in this direction, in line with the loading force, is investigated.

The loading force introduces three kinds of deformation types in the flexure: compression, shear, and bending. Due to these deformations, the deflection angle of the flexure changes. This is not allowed, as the rotation of the endpoint of the flexure is constrained by the attached system. This constraint results in an additional moment at the endpoint of the flexure. For each of these deformation types, linear beam theory prescribes an equation for its stiffness. These equations show that the support stiffness is dependent on the diameter, length, material stiffness, and Poison's ratio. However, the maximum strain a material allows also indirectly influences the support stiffness, as it defines the ratio between thickness and length of the flexure for a given range of motion.

3.2 Influence Of Strain On Flexure Geometry

The amount of strain in a flexure is dependent on the length, thickness, and deflection angle of a flexure. For a bent flexure as can be seen in figure 6, the following can be found. A thicker flexure of the same length increases strain, as both the stress and strain increases linearly away from the neutral axis of the flexure. Contrarily, a longer flexure decreases strain, as the bend is spread out over a longer distance. Therefore the length over radius ratio of the flexure L/r is investigated, and how the amount of strain that is allowed in a material limits this ratio.

When bending a flexure, the outer sides have the highest amount of strain. The neutral axis for the wire flexure, which is the axis which does not see any strain or longitudinal forces during bending, lies in the centre of the flexure. This neutral axis then also does not change in length during bending. From this, the strain in the material at the outer sides can be found by rewriting the formula for strain:

$$\varepsilon_{max} = \frac{dL_{max}}{L} = \frac{L_{max} - L}{L} \tag{1}$$

As the flexure forms a circular arc, the arc length of a flexure is equal to $L_{arc} = R\phi$. The L_{max} of the flexure can be rewritten as:

$$L_{max} = \phi(R + r) = L + r\phi \tag{2}$$

Filling this into the equation 1 gives:

$$\varepsilon_{max} = \frac{L + r\phi - L}{L} = \frac{r\phi}{L} \tag{3}$$

We define the maximum allowed strain as the maximum strain before yielding. This maximum strain is given by $\varepsilon_{allowed} = YS/E$. In literature, this strain is also called elongation at yield, or elasticity percentage. Combining this maximum strain with equation 3 results in equation 4. In this equation, only strain by bending is taken into account. External forces can cause additional strain in the flexure, requiring either a thinner or longer flexure. As this is dependent on the use case of the flexure, it is not taken into account here.

$$\frac{L}{r} = \frac{\phi_{max}}{\varepsilon_{allowed}} \tag{4}$$

From equation 4 it can be seen that for a certain deflection angle of the flexure, a material with a higher maximum strain allows a larger diameter for the same length. This means that materials that allow more strain but have a lower young's modulus can still result in a higher support stiffness. To test this theory, a material that allows one of the highest amount of strain is looked at, polyurethane [7]. Polyurethane can stretch up to 100% without yielding, while for steel this is only about 0.5%. For the tests in this paper, a 3D printable TPU is used with a maximum strain of 55% [8], still a factor 110 larger than steel. This results in a wire flexure with a diameter that is also 110 times larger, or D_{ratio} = 110. However, the Young's modulus of TPU is a lot

TABLE 1: Stiffness ratio of steel over TPU for each deformation mode based on linear beam theory, showing the stiffer TPU, especially in bending. D_{ratio} and E_{ratio} are the ratio between two materials' diameter and Young's modulus, respectively

Deformation mode	Stiffness ratio equation	$\frac{TPU}{Steel}$
Compression	$D_{ratio}^2 \cdot E_{ratio}$	1.6
Shear	$D_{ratio}^2 \cdot E_{ratio} \cdot \frac{1+\nu_1}{1+\nu_2}$	1.7
Bending	$D_{ratio}^4 \cdot E_{ratio}$	1.9×10^4

lower than steel, 26 MPa vs 200 GPa, respectively. This difference is approximately a ratio of $E_{ratio} = 1.3 \times 10^{-4}$. Finally, the Poisson's ratio of steel is 0.28 and for TPU 0.4. The stiffness differences for each deformation mode can now be calculated based on the equations from linear beam theory, as is shown in table 1. TPU is stiffer in each deformation mode, which results in a higher total support stiffness of the flexure. How much higher exactly is based on how each deformation mode influences the total support stiffness of the flexure, as especially bending stiffness is higher for TPU. To find the ratio between each of the deformation modes, and how they change for different deformation angles, a model is made for the support stiffness of the wire flexure.

3.3 Modelling Support Stiffness

A model for the support stiffness could be based on testing in a tensile testing machine or modelling in a FEM program. However, to create an understanding for how much a certain parameter influences the support stiffness, many parameter studies would need to be performed. Instead, a model is created based on linear beam theory, which can then be checked against FEM programs. As stated in section 3.1, the force introduces compression, shear and bending on the flexure. The contribution to the support stiffness of each of the deformation types changes for different deflection angles of the flexure. For very small deflection angles, the force almost solely introduces compression in the flexure and thus the support stiffness will be dominated by the compression stiffness, or limited by buckling. For large deflection angles, compression in the flexure decreases while bending and shear increase. If the ratio between each of these aspects is known, also the effect of each design parameter on the support stiffness can be determined. This can be taken into account to optimise flexure designs for high support stiffness.

To calculate these ratios, a finite element model is made. The difference with a simulation in a FEM program is that the model in this paper is specific to the calculation of support stiffness, giving both more control and showing in more detail the effect of each parameter on the support stiffness. The wire flexure is split up in small elements along the flexure of size $d\theta$, and

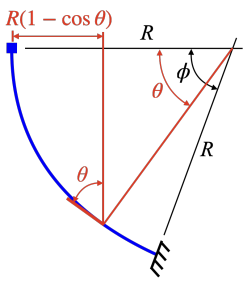

(a) The moment arm $R*(1-\cos\theta)$ and angle θ of the loading force on an element along the bend flexure.

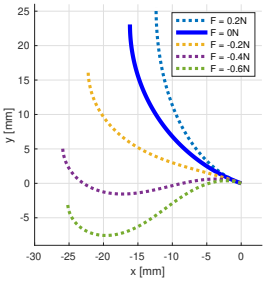

(b) Different loading forces on a bend steel flexure with a length of 30 mm and diameter of 0.25 mm, bent to 70°.

FIGURE 7: Support stiffness modelling approach

for each, the deflection from each contribution is calculated. In this model, each element is approximated as a circular arc, similar to Chen [9]. The amount of each deformation type changes along the flexure. At the tip, the force is in line with the flexure, resulting in pure compression. From figure 7a it can be seen that at the base, the force has both an angle ϕ and a moment arm of $R*(1-\cos\phi)$, increasing deflection from shear and bending but decreasing from compression. Any point in between at angle θ has the force at this angle θ and a moment arm of $R*(1-\cos\theta)$.

Each deformation type has a different effect on a small element. Compression changes the arc length of the element. Shear shifts two elements with respect to each other. Shear is modelled by rotating each element by its shear angle γ. The moment caused by the force is added to the already existent bending moment in each element, changing the radius of curvature. It is not taken into account yet, that the deflection angle is constrained by the attached system. This adds an additional moment on the flexure as is shown in figure 5. As only bending causes a change in rotation of the flexure, the bending moment in each element can be integrated over the length of the flexure, and added to the endpoint of the flexure. To increase accuracy for large deformations, the model can be looped to include the effect of deflection increasing the moment arm in the flexure, which in turn increases deflection, as shown in figure 7b.

From this model can indeed be seen that the effect of compression decreases while bending and shear increase. This is true for every flexure, as it is coupled to how the force interacts with the flexure, not the wire flexure geometry or material. However, the ratio between compression, shear and bending do change with different geometry or material constants, and so does the total support stiffness of the flexure. The results for a TPU and steel flexure are given in section 4.2

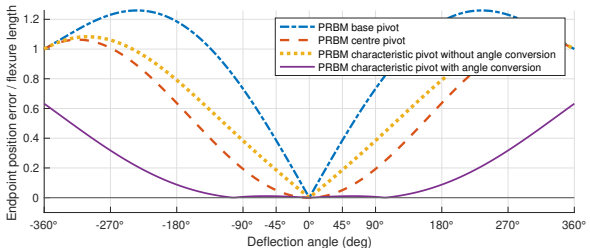

FIGURE 8: The normalised error of endpoint calculated by the different PRBM methods against the actual flexure deformation calculated with the arc method plotted over the deformation angle. The PRBM methods without an angle coefficient all have an error of 1 at 360°, meaning a full flexure length of error. This is because the arc method correctly predicts that the flexure shape creates a loop at 360° deflection, having the endpoint and base of the flexure touch, while the circle paths of the PRBM methods rotate back to their starting position. Hence, a flexure length of error.

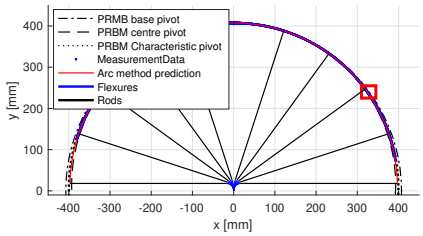

FIGURE 9: The position of the endpoint of a rod attached to a 3D printed TPU flexure, with a few flexure and rod positions drawn in. The flexures are drawn in blue at the bottom centre of the figure, with the black rods extending from the flexures. Also drawn are the PRBM paths for each of the three rotation points. The flexure is made from TPU, has a diameter of 15 mm and a length of 25 mm. The rod has a length of 380 mm. A zoomed in view of the red rectangle is given in figure 10

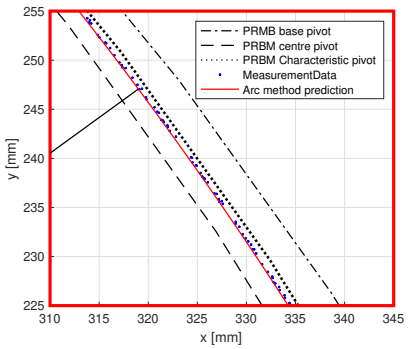

FIGURE 10: A zoomed in section from the red rectangle from figure 9. Here the difference between the path of the three PRBM methods and that of the arc method with respect to the measurement data can be seen.

4 RESULTS

In section 2 and 3, two models are developed for the short wire flexure, for which the results are presented in this section. The first model shows the axis drift and flexure shape of the short wire flexure, of which the results are given in section 4.1. The model is compared against PRBM, and checked against a FEM program. Finally, the method is measured against a physical test by deflecting a polyurethane wire flexure whilst measuring its position and rotation. The second model shows the support stiffness and the effects of different flexure parameters on this stiffness. The results of this model are given in section 4.2. The model is then checked by comparing the total support stiffness to results from FEM programs.

4.1 Arc Method Results

The results of the arc model are checked against data from COMSOL Multiphysics®. Both the 2D beam mechanics and the 3D solid mechanics interfaces are used. If a moment is placed on a beam in the beam mechanics interface, the path of the endpoint matches within 0.01% with the arc method over a deflection of 360°. The path for the 3D model of the steel flexure matches within 0.1%. The 3D model of a TPU Flexure matches closely for small deformations, but the error increases as the deflection angle increases. For a deformation angle of 50°, the error is 1.9%.

In figure 8, the error of each of the PRBM methods with respect to the arc method is calculated. Three PRBM methods are compared, each with a different pivot location. These PRBM methods can also be seen in figure 4. The error is calculated by taking the distance between the endpoint of each method for a given deflection angle. Figure 8 also shows that when the characteristic pivot PRBM is used with the angle coefficient, high accuracy for modelling the endpoint is reached for angles up to 124.4°. Do note that this accuracy is for the endpoint of the flexure, as the angle coefficient introduces an error for the attached system as discussed in section 2.3. If the angle coefficient is not used, the error is higher than that of the PRBM approximation with centre pivot.

The arc method is tested against measurements done on a TPU flexure hinge such as in figure 1a. Here the endpoint position of a rod attached to the TPU Flexure is measured over a large deflection range of ±70° as is shown in figure 9. In this figure, the test data is shown, as well as the PRBM and arc method. A zoomed-in view of this data can be found in figure 10, where the differences between the methods can be seen in more detail.

The error of the measured data with respect to the arc method is shown in figure 11. The maximum error is found at the largest deformation angles, ≈ 0.4 mm error at ±70°. The trend

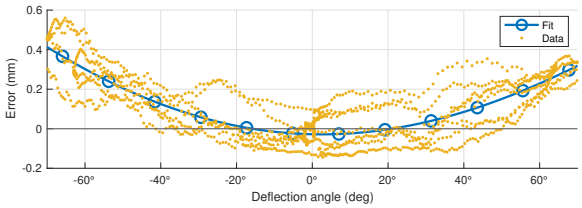

FIGURE 11: Error of the tested data to the arc method predictions. A positive error means the measurement data lies outside of the arc method. The smoothing spline fit shows a maximum error of 0.4 mm at 70°

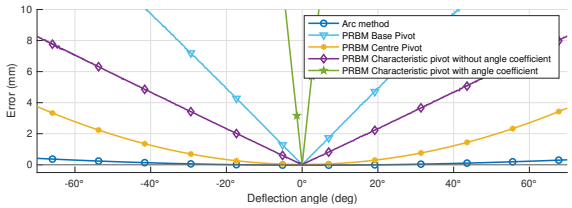

FIGURE 12: The error of the PRBM and arc method. At 70°, the arc method shows a factor 10 lower error than most accurate PRMB, which is the centre pivot PRBM. The characteristic pivot performs worse even though the path seems to match better, as the angle is also taken into account. Each of the lines is a fitted average of the data using a smooth spine fit. PRBM base pivot and Characteristic pivot with angle conversion continue linearly to $\pm 70°$.

of the data shows however a drift in this error. While the arc method matches for small angles, for large angles the measured data is outside of the arc method prediction. However, to put this error into perspective, it is compared against the error of the different PRBM. The results of this comparison can be found in figure 12. The smallest error of a PRBM method at these $\pm 70°$ is ≈ 4 mm, a factor 10 more. The PRBM method with characteristic pivot shows larger error than the centred PRBM, even though the path seems to match better as can be seen in figure 10, as the deflection is also taken into account when calculating the error.

4.2 Support Stiffness Results

The support stiffness model from section 3.3 is used to model the stiffness of a steel flexure and a TPU flexure over a range of bend angles, as shown in figure 13.

Figure 13 also shows how at an deflection angle of 0° the ratio between the support stiffness is 1.6, comparable to the difference in pure compression stiffness as stated in table 1. At large deformation angles, this ratio quickly increases, to approximately 7800 at 70°. To see what parameters affect this stiffness, the contribution of each deformation type to the total compliance of the flexure is investigated, which can be seen in figure 14.

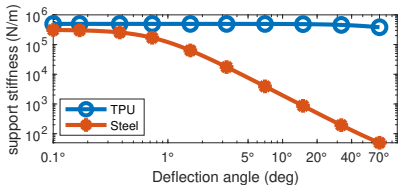

FIGURE 13: The support stiffness of a steel and TPU wire flexure for different bend angles. From an angle of 1°, the support stiffness of the steel flexure drops, until a ratio of 7800 at 70°. Each has a diameter that corresponds to a length of 30 mm and a maximum bend angle of 70°. For steel this is a diameter of 0.25 mm, for TPU it is 27 mm

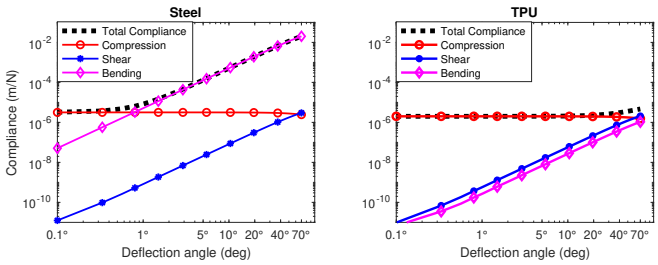

FIGURE 14: The contribution of compression, shear and bending to the total compliance for a steel and TPU Flexure, plotted for different deflection angles. The compliance of the steel flexure increases due to the low bending stiffness to 10^{-2} at 70° The compliance of the TPU flexure stays at 10^{-6}.

Do note that figure 13 and 14 only show the instant support stiffness calculated by the support stiffness model, not taking into account the non-linear loading behaviour of the flexure. Especially with the thin steel flexure, this behaviour causes a decrease in stiffness when the flexure is compressed. When the loading force deforms the flexure, the moment arm of this force is increased, which then increases deformation again. This behaviour is seen in figure 15.

The results of the support stiffness model are checked against data from COMSOL MultiPhysics®. Both the 2D beam mechanics and the 3D solid mechanics interfaces are used. The models match within 0.1% with the data from the beam interface for both TPU and steel, for a large deflection range as shown in figure 15. The 3D steel flexure also matches with the support stiffness model. However, the deflection results from the TPU flexure in the solid mechanics interface do deviate from the support stiffness model at large deflections. The instant stiffness does match within 0.1%, but as soon as the flexure starts deforming, the error increases. This error ranges from 1% at a compression force of 10 N giving a deflection of 0.1 mm, to 14% at 100 N giving a deflection of 1.2 mm.

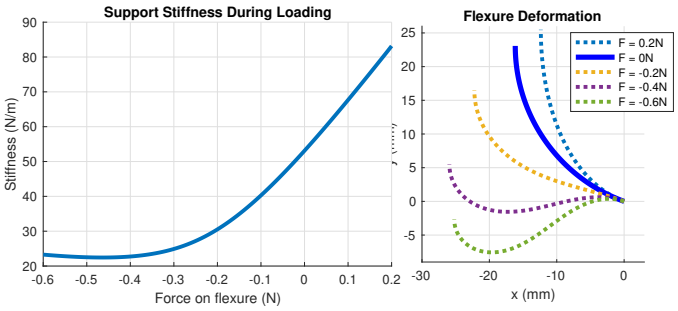

FIGURE 15: The support stiffness behaviour of a steel wire flexure during loading. On the left, the drop in stiffness for higher loading forces, caused by the increased moment arm which is shown the right.

5 DISCUSSION

5.1 The Arc Method

The measurement results show the arc method has higher accuracy than the existing PRBM methods. However, figure 11 shows a mismatch between the predicted path by the arc method and that of the flexure. At large deflections especially, the data lies outside of the predicted curve by the arc method. For this to happen, the flexure either has to increase in arc length or not follow a circular arc. It is not likely that the flexure deviates from the circular arc, as the bending moment, shape, and material are the same over the length of the flexure. That means that the flexure increases in arc length, thus elongates while deforming. This could be caused by a difference in compression vs tension behaviour in the flexure. If the TPU used for the flexure is stiffer in compression than it is in tension, a bending moment will cause the flexure to elongate. A difference in creep or hysteresis between tension and compression could also be the cause, as this gives the same effect as the difference in stiffness. The flexure for the tests was 3D printed, which could also further introduce non-linear material effects.

The measurement results also show the effect of the endpoint angle error introduced by the angle coefficient for the characteristic pivot. This method only works up to the endpoint of the flexure, not taking into account any systems that attach to it. An additional bend could be added to the endpoint of the flexure, bending back to the original angle. However, this increases complexity, as the distance between the PRBM pivots is now not constant anymore, but changes for different deflection angles. Just as with the arc method and VC, this can result in a necessity for an iterative solver when solving a system with multiple flexures. Another possible option is to match the angle coefficient and characteristic pivot not for the flexure itself, but for the flexure and attached rod together. This could work for a single joint, but in systems with multiple joints this also increases complexity. Based on this, two options arise for modelling flexure systems. Of the less complex methods with a fixed single pivot, the PRBM model with a centre pivot has the lowest error. If high accuracy is required, the arc method has a tenth of the error of PRBM, but a higher complexity due to the shifting pivot location.

5.2 Support Stiffness

The support stiffness model shows a large increase in support stiffness for the TPU flexure with respect to the steel flexure, mainly because of the large increase in bending stiffness for the TPU flexure. The deformation of the steel flexure is quickly dominated by deformation due to bending. For the TPU flexure, due to the larger diameter and thus high area moment of inertia, the contribution to the deflection of compression and shear are larger than that of bending.

The support stiffness model overall matches the results from COMSOL Multiphysics® closely, only for large deflections of the TPU flexure the error increases. This is likely caused by the behaviour of the flexure at the attachment points and effects like anticlastic curvature, which are not taken into account in the support stiffness model, but are modelled in COMSOL Multiphysics®.

5.3 Applications Of The Methods

Both the support stiffness model and arc method are now focused on the short wire flexure, but are not limited to only that application. Using high strain materials such as polymers to increase support stiffness can be applied to other flexure types, as each of the deformation types is stiffer for TPU with respect to that of steel. The exact increase in support stiffness is dependent on the application, as the bending mode shows the largest stiffness difference.

5.4 Material Assumptions

The TPU used in this paper was assumed to be a homogeneous material with linear material behaviour. Polymers also suffer from high creep, which also was not taken into account in this paper. The test samples used in this paper were 3D printed, limiting the quality of material possible. Using injection moulding could result in higher yield over Young's modulus, resulting in shorter and thicker flexures, giving even higher stiffness. Polymers have higher internal friction than steel, which combined with the larger strain could result in heating of the flexures, changing material constants. This large internal friction can also act as internal damping, reducing the vibrations in the system. Next to this, flexures from combinations of different materials such as a steel core and polymer outside could even further increase precision and accuracy of flexure systems.

6 CONCLUSION

This paper presents a simple analytic model for the axis drift of wire flexures for large ranges of motion. This model, named the arc method, models the flexure as a circular arc, based on the deformation by a pure moment. A virtual centre is defined to more efficiently include the arc method in kinematic models, as it simplifies the system to a single rotation point per deflection angle of the flexure.

The arc method is validated by comparing it to FEM and a physical test, both showing good agreement. Different PRBM methods are also compared against the measurement data, showing a factor 10 larger errors than the arc method at deflections of 70°.

Next to this, this paper shows how the use of polymers can increase precision and robustness of a short wire flexure. The diameter of a flexure is defined by the maximum allowed strain and required deflection angle. Based on this, the large allowed strain of polymers results in a larger diameter than steel for the same bend angle.

The support stiffness model from this paper shows how polymers increases support stiffness even though the material stiffness is substantially lower than that of steel. This model also shows the influence of the different deformation types on the support stiffness of a bent flexure. This gives the possibility to increase support stiffness by optimising the stiffness of each deformation type.

The support stiffness model is validated by comparing it to FEM showing a maximum error of 0.1% to the 2D beam interface, and a matching instant stiffness for the 3D solid mechanics interface.

To conclude, combining high support stiffness from polymers with the arc method can result in flexures with high precision and accuracy while having a simple geometry such as a wire flexure.

REFERENCES

[1] Larry L. Howell. *Compliant mechanisms*. Wiley, 2001.

[2] M. Naves, D. M. Brouwer, and R. G. K. M. Aarts. Building Block-Based Spatial Topology Synthesis Method for Large-Stroke Flexure Hinges. *Journal of Mechanisms and Robotics*, 9(4), 8 2017.

[3] D. Farhadi Machekposhti, N. Tolou, and J. L. Herder. A Review on Compliant Joints and Rigid-Body Constant Velocity Universal Joints Toward the Design of Compliant Homokinetic Couplings. *Journal of Mechanical Design*, 137(3), 3 2015.

[4] Brian P. Trease, Yong-Mo Moon, and Sridhar Kota. Design of Large-Displacement Compliant Joints. *Journal of Mechanical Design*, 127(4):788, 7 2005.

[5] I. Gustavsson, L. Ljung, and T. Söderström. Identification of processes in closed loop—identifiability and accuracy aspects. *Automatica*, 13(1):59–75, 1 1977.

[6] Zhonglei Feng, Yueqing Yu, and Wenjing Wang. Modeling of large-deflection links for compliant mechanisms.

[7] GRANTA EduPack — Granta Design.

[8] Ultimaker TPU 95A material: 3D print durable and flexible parts.

[9] Guimin Chen, Fulei Ma, Guangbo Hao, and Weidong Zhu. Modeling Large Deflections of Initially Curved Beams in Compliant Mechanisms Using Chained Beam-Constraint-Model. 2018.